Journal of Alloys and Compounds 509 (2011) 1389–1393

Contents lists available at ScienceDirect

Journal of Alloys and Compounds

journal homepage: www.elsevier.com/locate/jallcom

Kinetic arrest behavior in martensitic transformation of NiCoMnSn metamagnetic shape memory alloy

R.Y. Umetsu[a,*], K. Ito[b], W. Ito[b], K. Koyama[c,1], T. Kanomata[d], K. Ishida[b], R. Kainuma[b]

[a] Institute for Materials Research, Tohoku University, 2-1-1 Katahira, Sendai 980-8577, Japan
[b] Department of Materials Science, Graduate School of Engineering, Tohoku University, 6-6-02 Aoba, Sendai 980-8579, Japan
[c] High Field Laboratory for Superconducting Materials, Institute for Materials Research, Tohoku University, Sendai 980-8577, Japan
[d] Faculty of Engineering, Tohoku Gakuin University, Tagajo 985-8537, Japan

ARTICLE INFO

Article history:
Received 3 June 2010
Received in revised form 27 October 2010
Accepted 28 October 2010
Available online 9 November 2010

Keywords:
Nickel alloys
Magnetic properties
Martensitic phase transformation
Shape memory alloys
Field-induced reverse martensitic transformation

ABSTRACT

High-field magnetic measurements were carried out in order to investigate behaviors of field-induced reverse martensitic transformation and kinetic arrest of NiCoMnSn metamagnetic shape memory alloy. In the thermomagnetization curves, it was confirmed that the reverse martensitic transformation temperature decreases 67 K by applying magnetic field of 5 T, while in the magnetic field cooling process under 5 T, martensitic transformation does not occur down to low temperatures. Equilibrium magnetic field, defined from the critical magnetic fields of the metamagnetic evidence in the magnetization curves, exhibits almost constant below about 100 K, suggesting that the entropy change becomes zero, which is considered to cause kinetic arrest behavior.

An unusual type of ferromagnetic shape memory alloy (FSMA) has been found in NiMnX (X = In, Sn, and Sb) Heusler alloys, where the martensite phase shows considerable weaker magnetism than that of the parent phase [1]. Thus, a drastic change in magnetization can be obtained during the martensitic transformation [2–4]. Application of a magnetic field significantly decreases the martensitic transformation temperature, and magnetic field-induced reverse martensitic transformation (MFIRT), namely, metamagnetic phase transformation, has also been confirmed in the temperature region below the reverse martensitic transformation starting temperature, T_{As}, in the NiMnX and NiCoMnX alloys [5–9]. Moreover, since these Ni-based FSMAs exhibit other very interesting physical properties, such as an almost perfect metamagnetic shape memory (MMSM) effect [6,7], a giant magnetoresistance effect [10–12] and an inverse magnetocaloric effect [13–15], these alloys have received much attention as high performance multiferroic materials.

Recently, a kinetic arrest (KA) phenomenon has been reported in NiCoMnIn [16,17], NiMnIn [18,19], NiCoMnGa [20] and NiCoMnAl alloys [21]. In that phenomenon, since martensitic transformation is interrupted at certain temperatures (noted as KA temperature, T_{KA}) during magnetic field cooling and does not proceed with further cooling, the parent phase remains down to low temperatures. The KA phenomenon has been confirmed by the abnormal critical magnetic field–temperature (H_0–T) [16,18,20,21] and critical stress–temperature (σ_0–T) [22] dependences to be caused by disappearance of the entropy change between the parent and the martensite phases at around T_{KA}. Although such a peculiar behavior of the entropy change would be associated with the magnetic contribution to the Gibbs energy of the parent phase, the origin is still under discussion. In this paper, for NiCoMnSn alloys, which are another type of the metamagnetic shape memory alloys [7], details on the MFIRT detected using high magnetic fields up to 12 T are reported and the KA phenomenon is confirmed.

Polycrystalline $Ni_{37}Co_{11}Mn_{42.5}Sn_{9.5}$ and $Ni_{37}Co_{11}Mn_{43}Sn_9$ alloys were made by induction melting under an argon atmosphere. Obtained ingots were annealed at 1173 K for 1 day for homogenization and then quenched into ice water. Powdered specimens for X-ray diffraction with Cu $K\alpha$ radiation were prepared by grinding the annealed specimens, where in order to remove the introduced strain, final annealing for the powdered specimens was carried out at 1173 K for 1 min. Thermal analyses were performed by differential scanning calorimetry (DSC) at heating and cooling rates of 10 K/min. Thermomagnetization curves were measured by

* Corresponding author. Tel.: +81 22 215 2492; fax: +81 22 215 2381.
E-mail address: rieume@imr.tohoku.ac.jp (R.Y. Umetsu).
[1] Present address: Graduate School of Science and Engineering, Kagoshima University, 1-21-35 Korimoto, Kagoshima 890-0065, Japan.

0925-8388/$ – see front matter © 2010 Elsevier B.V. All rights reserved.
doi:10.1016/j.jallcom.2010.10.176

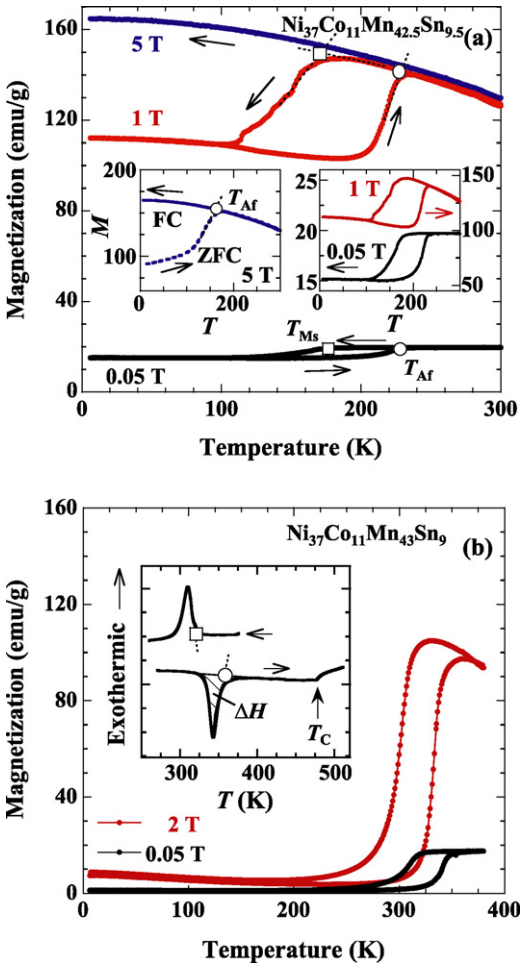

Fig. 1. (a) and (b) Thermomagntization (M–T) curves of the $Ni_{37}Co_{11}Mn_{42.5}Sn_{9.5}$ alloy under the magnetic fields of 0.05, 1 and 5 T. The measurements were started at 300 K and the temperature was scanned between 300 and 6 K under a certain magnetic field. Inset (left hand) shows the zero-field cooled (ZFC) and field cooled (FC) M–T curves, in which the ZFC curve was measured during heating in a magnetic field of 5 T after zero-field cooling. Inset (right hand) indicates large scale of the M–T curves of 0.05 and 1 T. Open circles and squares indicate reverse martensitic transformation finishing temperature, T_{Af}, and martensitic transformation starting temperature, T_{Ms}, respectively. (b) M–T curves of the $Ni_{37}Co_{11}Mn_{43}Sn_9$ alloy in the magnetic fields of 0.05 and 2 T. Inset shows the DSC heating and cooling curves.

a SQUID magnetometer at heating and cooling rates of 2 K/min and the magnetization as a function of magnetic fields was measured by an extraction-type magnetometer using a superconducting magnet installed in the High Field Laboratory for Superconducting Materials, Institute for Materials Research, Tohoku University.

Thermomagnetization (M–T) curves of the $Ni_{37}Co_{11}Mn_{42.5}Sn_{9.5}$ alloy in the magnetic fields of 0.05, 1 and 5 T are shown in Fig. 1(a), where all the measurements were started at 300 K and the temperature was scanned between 300 and 6 K under a certain magnetic field. On the other hand, the M–T curves, taken from the same specimen heated to 300 K under a magnetic field of 5 T after cooling down to 6 K under zero-magnetic field (ZFC) and then further cooled under the same magnetic field (FC), are exhibited in the inset of Fig. 1(a). In both the figures, open circles and squares indicate the reverse martensitic transformation finishing temperature, T_{Af}, and the martensitic transformation starting temperature, T_{Ms}, respectively. It is seen that the T_{Af} of 0.05 T at about 229 K drastically decreases to 162 K by the application of the magnetic field of 5 T. On the contrary, in the FC of 5 T, no martensitic transformation is detected to 6 K. This behavior is caused by stabilization of the parent phase due to the application of a magnetic field and suggests the KA phenomenon as reported in the other MMSM alloys [16–21]. In the present alloy system, comparatively higher amount of Co element could be substituted for Ni than in the NiCoMnIn system [23]. Consequently, magnetic properties of the ferromagnetic parent phase are enhanced, and for the $Ni_{37}Co_{11}Mn_{42.5}Sn_{9.5}$ alloy, the magnetization at 4.2 K reaches about 160 Am^2/kg (7.2 μ_B/f.u.) and the Curie temperature becomes about 478 K. Furthermore, the decrease of martensitic transformation temperatures induced by magnetic field in the present alloy seems to be larger than that in the $Ni_{45}Co_5Mn_{36.5}In_{13.5}$ alloy [24]. Fig. 1(b) indicates the M–T curves obtained under the magnetic fields of 0.05 and 2 T for the $Ni_{37}Co_{11}Mn_{43}Sn_9$ alloy with a slightly lower Sn composition, the inset showing the DSC heating and cooling curves. From the DSC curves, the T_{Af}, T_{Ms} and the Curie temperature, T_C, are confirmed to be 352, 318 and 477 K, respectively. Comparing the M–T curves of the two specimens, a considerable difference is noticed in the magnetization of the martensite phase, i.e., that in the $Ni_{37}Co_{11}Mn_{42.5}Sn_{9.5}$ alloy is significantly higher than that in the $Ni_{37}Co_{11}Mn_{43}Sn_9$ alloy. This fact means that in the $Ni_{37}Co_{11}Mn_{42.5}Sn_{9.5}$ alloy (Fig. 1(a)) the parent phase remains even at temperatures below 100 K and the T_{KA} is about 100 K, where the T_{KA} is defined as the temperature at which the heating and cooling curves coincide [21]. As shown in the inset (right hand) of Fig. 1(a), in which the M–T curve of 0.05 T is enlarged and compared with that of 1 T, the T_{KA} in both the curves are almost the same, and field dependence of the T_{KA} is hardly detected. The transformation enthalpy, ΔH_{Ent}, can be evaluated from the thermal analysis as shown in the inset of Fig. 1(b). The obtained result is discussed below.

Fig. 2 shows the X-ray powder diffraction (XRD) patterns measured at 300 and 8 K for $Ni_{37}Co_{11}Mn_{42.5}Sn_{9.5}$ alloy (a) and at about 340 K and RT for $Ni_{37}Co_{11}Mn_{43}Sn_9$ alloy (b), together with calculated patterns. Fig. 2(c) displays the partial spectrum of (b) with an expanded scale. For the $Ni_{37}Co_{11}Mn_{42.5}Sn_{9.5}$ alloy, both the XRD patterns of 300 and 8 K are indexed as an $L2_1$-type structure with lattice constants of $a = 0.5950$ and 0.5937 nm, respectively. Here, an unknown peak marked with cross at around $2\theta = 48^\circ$ is due to the background associated with the facilities. No martensite phase is detected in this powdered specimen of $Ni_{37}Co_{11}Mn_{42.5}Sn_{9.5}$, although the bulk specimen with the same composition does exhibit a martensitic transformation at low temperature as shown in Fig. 1(a). The reason of disappearance of the transformation is not clear, but this would be caused by a kind of size effects. When specimen size is very small, nucleation of martensite plates may be harder than that in polycrystalline bulk specimen including many lattice defects acting for nucleation sites. Surface oxide layer formed during the final annealing may also make the parent phase stabilize due to mechanical constraint against martensitic transformation. Reduction of martenstic transformation temperatures due to decrease of particle size have been reported in many other materials such as Fe–Ni, Ti–Ni and ZrO_2 [25–27]. As shown in Fig. 2(b), the XRD patterns at about 340 K and RT obtained for the $Ni_{37}Co_{11}Mn_{43}Sn_9$ alloy are completely different because of the appearance of the martensite phase. The T_{Af} of the powdered specimen of $Ni_{37}Co_{11}Mn_{43}Sn_9$ is 342 K and 10 K lower than that of the bulk specimen (see the inset of Fig. 1(b)), thus, the peaks associated to the martensite phase slightly remains in the diffraction measured at about 340 K. According to our previous research using transmission electron microscopy (TEM), the structure of the martensite phase in $Ni_{43}Co_7Mn_{39}Sn_{11}$ is characterized as a mixture of 10- and 6-layered monoclinic type structures, i.e., 10M- and 6M-type structures, which are denoted as $(3\bar{2})_2$ and $(4\bar{2})$ in Zhdanov notation, respectively [7]. If the 10M- and 6M-type structures have the same stacking unit as one of the distorted $L2_1$ (namely, fct) phases, the lattice constants for the 10M- and 6M-

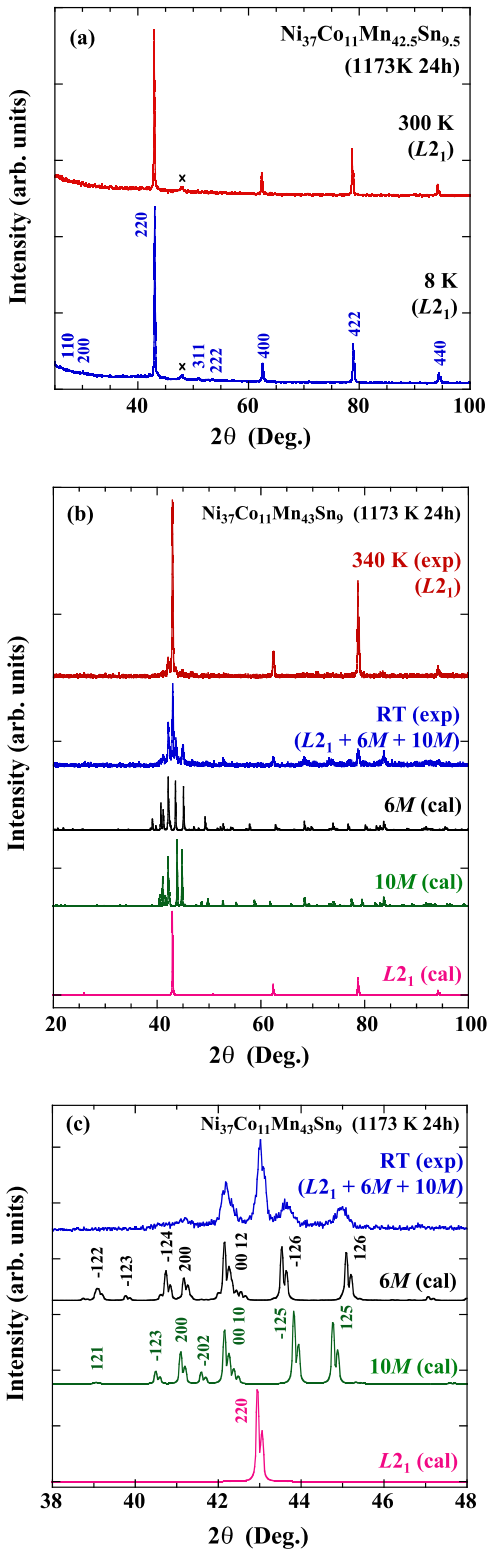

Fig. 2. X-ray powder diffraction (XRD) patterns measured at 300 and 8 K for $Ni_{37}Co_{11}Mn_{42.5}Sn_{9.5}$ alloy (a) and at about 340 K and RT for $Ni_{37}Co_{11}Mn_{43}Sn_9$ alloy (b), together with calculated patterns, and (c) is the partial spectrum of (b) with in expanded scale.

type structures can be easily evaluated on the basis of the 2*M* structure possessing a lattice correspondence with the fct structure as $a_{2M} = c_{2M} = (\sqrt{a_{fct}^2 + c_{fct}^2})/2$ and $b_{2M} = a_{fct}$ [28]. In the present study, the lattice constants of the fct structure, $a_{fct} = 0.5487$ and $c_{fct} = 0.6880$ nm, were determined from some reflections independent of the layered sequence. The lattice constant of the parent phase with the $L2_1$ structure measured at 340 K is $a = 0.5952$ nm. This result means that the basic tetragonal distortions from the $L2_1$ phase due to the martensitic transformation are about −7.9% along the *a*-axis and about +15.6% along the *c*-axis, and that the volume change is about −1.8%. The monoclinic angle β of the stacking structures $(n\bar{m})_2$ can be evaluated as [28]:

$$\tan(\beta - 90^\circ) = A \cdot \tan(\beta_0 - 90^\circ), \quad (1)$$

where A ($\equiv(n-m)/(n+m)$) is a constant indicating the extent of deviation from 90° in the angle β, β_0 is the monoclinic angle of the 2*M* structure, and given as $A_{2M} = 1$, $A_{10M} = 0.2$ and $A_{6M} = 0.33$. Using the lattice correspondence as mentioned above, the lattice constants *a*, *b* and *c* for the 10*M*- and 6*M*-type structures are also primarily refined from the lattice constants of the 2*M* structure as $a_{10M} = a_{6M} = a_{2M}$, $b_{10M} = b_{6M} = b_{2M}$, $c_{10M} = 5c_{2M}$ ($\sin\beta_0/\sin\beta_{10M}$) and $c_{6M} = 6c_{2M}$ ($\sin\beta_0/\sin\beta_{6M}$). As shown in Fig. 2(c), the experimental pattern can be completely indexed as a mixture of the 10*M*- and 6*M*-type structures with the lattice constants of $a_{10M} = 0.4400$ nm, $b_{10M} = 0.5487$ nm, $c_{10M} = 2.1472$ nm, $\beta_{10M} = 92.61^\circ$, and $a_{6M} = 0.4400$ nm, $b_{6M} = 0.5487$ nm, $c_{6M} = 2.5812$ nm, $\beta_{6M} = 94.31^\circ$, respectively and these values are listed in Table 1. The results obtained from the XRD patterns are comparable to the structures determined by the TEM observations [7].

Fig. 3(a) and (b) shows the magnetization (*M*–*H*) curves measured at various temperatures for the $Ni_{37}Co_{11}Mn_{42.5}Sn_{9.5}$ alloy, where the *M*–*H* curves were obtained by the cyclic measurement inserting a heating process in every interval to fix the initial condition in every curve. In all the *M*–*H* curves except that of 4.2 K, a drastic and continuous change in magnetization associated with the MFIRT can be observed in the filed-applying process. On the other hand, in the field-releasing process, some depression of magnetization due to the forward martensitic transformation appears in the low magnetic field region in all the curves except those at 4.2 and 25 K. This means that at 4.2 and 25 K no forward martensitic transformation occurs in the field-releasing process. In the present study, the reverse martensitic transformation finishing magnetic field, H_{Af}, and the martensitic transformation starting magnetic field, H_{Ms}, are defined as the field at the intersection of the base line and the tangent line in the transformation region of the *M*–*H* curve, as indicated by the open circles and squares, respectively. The H_{Af} and H_{Ms} increase with decreasing the measured temperature in the temperature region to 100 K (Fig. 3(a)), and the transformation hysteresis, defined as $H_{Af} - H_{Ms}$, drastically increases with decreasing temperature in the region below 75 K (Fig. 3(b)). In addition, the steps in the *M*–*H* curve of 4.2 K apparently exhibit a burst transformation, which may be caused by the decrease of the mobility of the habit plane during the transformation. A similar behavior at very low temperatures has been reported in $Ni_{45}Co_5Mn_{36.7}In_{13.3}$ [16] and $Ni_{50}Mn_{34}In_{16}$ [18] alloys.

Let us define the equilibrium magnetic field, H_0, at which the parent phase and the martensite phase have an equal Gibbs free energy, as $H_0 = (H_{Ms} + H_{Af})/2$. Fig. 4(a) displays the H_{Ms}, H_{Af} and H_0 determined from the *M*–*H* curves of the $Ni_{37}Co_{11}Mn_{42.5}Sn_{9.5}$ alloy in Fig. 3(a) and (b) as a function of the measured temperature. Here, the square symbols indicate the T_{Af} and T_{Ms} determined from the *M*–*T* curves of the $Ni_{37}Co_{11}Mn_{42.5}Sn_{9.5}$ in Fig. 1(a), together with the equilibrium temperature T_0 defined as $T_0 = (T_{Ms} + T_{Af})/2$. The data of the transformation magnetic fields are coincident with those of the transformation temperatures. It is obvious that while increasing

Table 1
Lattice constants of the $L2_1$ phase and monoclinic stacking structures of $Ni_{37}Co_{11}Mn_{42.5}Sn_{9.5}$ and $Ni_{37}Co_{11}Mn_{43}Sn_9$ alloys.

Alloy	T (K)	Phase	Lattice constants, a (nm)
$Ni_{37}Co_{11}Mn_{42.5}Sn_{9.5}$	300 K	$L2_1$	$a = 0.5950$
	8 K	$L2_1$	$a = 0.5937$
	340 K	$L2_1$	$a = 0.5952$
$Ni_{37}Co_{11}Mn_{43}Sn_9$	RT	$L2_1$	$a = 0.5952$
		6*M*	$a = 0.4400$, $b = 0.5487$, $c = 2.5812$, $\beta = 94.31°$
		10*M*	$a = 0.4400$, $b = 0.5487$, $c = 2.1472$, $\beta = 92.61°$

with decreasing temperature in the high temperature region, the H_0 (T_0) becomes almost flat in the region below about 100 K. The Clausius–Clapeyron relation between magnetism and temperature is expressed as follows:

$$\frac{dH}{dT} = -\frac{\Delta S}{\Delta M}, \tag{2}$$

here, ΔS and ΔM being the transformation entropy change and the difference in magnetization between the parent and the martensite phases, respectively. If we assume simply that the ΔM is constant, there is a linear relation between ΔS and $-dH/dT$, that is, the slope of H_0 is proportional to the transformation entropy change. Therefore, in the temperature region with the constant H_0 below 100 K, the ΔS is evaluated as being zero. In the present case, the ΔM can be estimated as being around 150 Am^2/kg because the magnetization of the martensite phase is less than 10 Am^2/kg, as shown by the *M*–*T* curve of 2 T of Fig. 1(b), and the magnetization of the parent phase in the temperature region below 200 K is located between 150 and 165 Am^2/kg, as shown by the *M*–*T* curve of 5 T of Fig. 1(a). Fig. 4(b) shows the ΔS estimated using Eq. (1) from the fitted H_0 curve drawn in Fig. 4(a), together with the datum obtained from the DSC heating curve. Here, the ΔS was determined with $\Delta S = \Delta H_{Ent}/T_t$, where $T_t \equiv (T_{As}^{DSC} + T_{Af}^{DSC})/2$ as shown in the inset of Fig. 1(b). The datum determined by DSC measurement is located on the broken line extrapolated from the solid one obtained from the H_0–T curve as shown in Fig. 4(b). It is important to note that decreasing with decreasing temperature, the ΔS line intersects the *x*-axis at about 100 K, which corresponds to the T_{KA}.

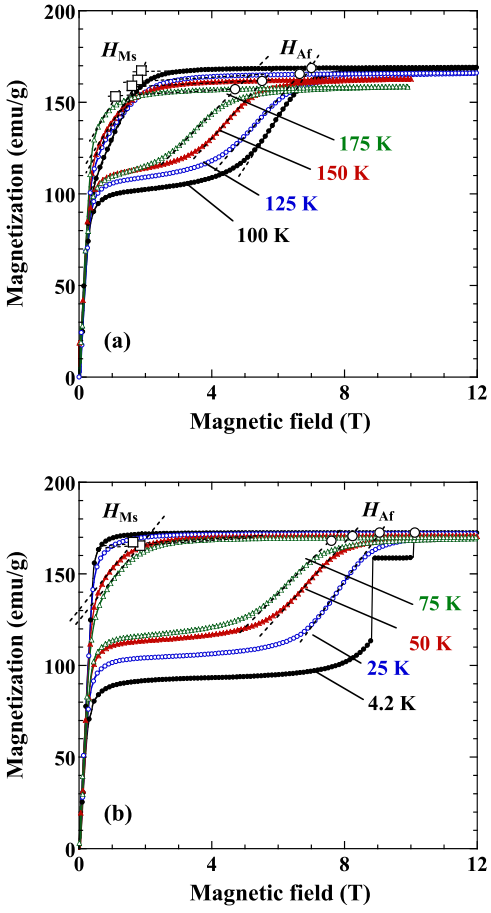

Fig. 3. (a) and (b) Magnetization (*M*–*H*) curves measured at various temperatures for the $Ni_{37}Co_{11}Mn_{42.5}Sn_{9.5}$ alloy, where the specimen was cooled down from 298 K to the examination temperature in no magnetic field and heated up to 298 K after measurement for every curve. (a) *M*–*H* curves at 100, 125, 150 and 175 K, and (b) *M*–*H* curves at 4.2, 25, 50 and 75 K. Open circles and squares indicate reverse martensitic transformation finishing magnetic field, H_{Af}, and martensitic transformation starting magnetic field, H_{Ms}, respectively.

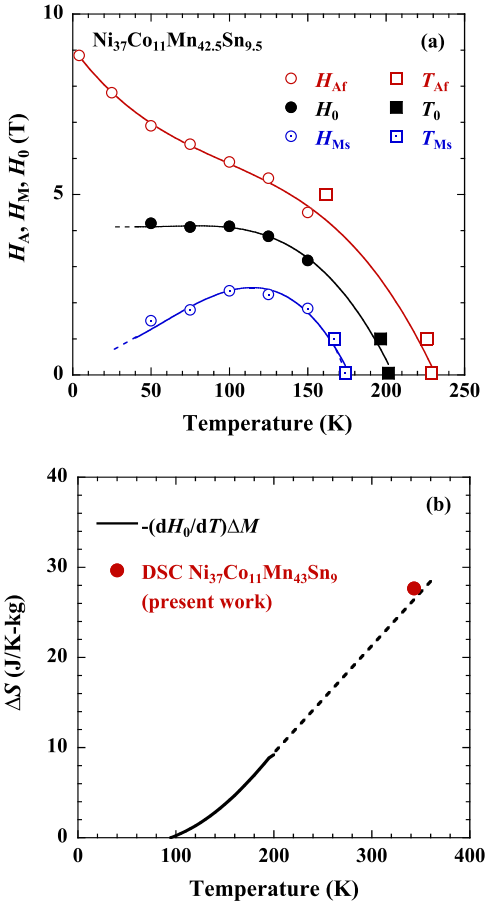

Fig. 4. (a) Temperature dependence of the equilibrium magnetic field H_0 obtained by the *M*–*H* curves. H_0 is defined as $H_0 = (H_{Ms} + H_{Af})/2$, and H_{Ms} and H_{Af} are the reverse martensitic transformation finishing magnetic field and martensitic transformation starting magnetic field, respectively. The square symbols indicate reverse martensitic transformation finishing temperature, T_{Af} and martensitic transformation starting temperature, T_{Ms}, determined from the *M*–*T* curves. T_0 is the equilibrium temperature, which is defined as $T_0 = (T_{Ms} + T_{Af})/2$. (b) Temperature dependence of the transformation entropy change ΔS for the $Ni_{37}Co_{11}Mn_{42.5}Sn_{9.5}$ alloy estimated using Eq. (1) from the fitted H_0 curve drawn in (a), together with the datum obtained from the DSC heating curve.

The KA behavior reported for the Ni-based FSMA [16–22] is understood to be due to the disappearance of the ΔS in the low temperature region, which would be strongly correlated with the magnetic contribution in the Gibbs energy of the ferromagnetic parent phase. For NiCoMnIn and NiMnIn alloys it was found that the ΔS approaches zero when $(T_C - T_{Ms})$ is larger than 200 K [16,17]. In other words, $(T_C - T_{Ms})$ is expected to be slightly larger than 200 K according to these reports and has been actually estimated to be about 255 and 225 K, respectively [16,18]. For the present NiCoMnSn alloy, $(T_C - T_{Ms})$ is about 310 K, larger than that for the NiCoMnIn and NiMnIn alloys. Since this difference has not been clarified yet, further investigations of the KA behavior in various alloy systems will be needed.

In summary, high-field magnetic measurements were carried out in order to investigate behaviors of the field-induced reverse martensitic transformation and of the kinetic arrest of $Ni_{37}Co_{11}Mn_{42.5}Sn_{9.5}$ metamagnetic shape memory alloy. In the thermomagnetization curves with the heating process after zero-magnetic field cooling, it was confirmed that the reverse martensitic transformation temperature decreases 67 K by applying magnetic field of 5 T, while in the magnetic field cooling process under 5 T, martensitic transformation does not occur down to low temperatures. Equilibrium magnetic fields, being defined from the critical magnetic fields of the metamagnetic evidence in the magnetization curves, exhibit almost constant below about 100 K, suggesting that the entropy change becomes zero, which is considered to cause kinetic arrest behavior.

Acknowledgments

The authors would like to thank Professors H. Morito and H. Yamane of Institute of Multidisciplinary Research for Advanced Materials, Tohoku University for helpful of the XRD measurements. This study was supported by Grant-in-Aids from Core Research for Evolutional Science and Technology (CREST), Japan Science and Technology Agency (JST) and from the Japanese Society for the Promotion of Science (JSPS), by a Grant-in-Aid for Scientific Research, and by the Global Center of Excellence (GCOE) Program "Materials Integration" (International Center of Education and Research), Tohoku University, MEXT, Japan. A part of this work was carried out at the Center for Low Temperature Science, Institute for Materials Research, Tohoku University.

References

[1] Y. Sutou, Y. Imano, N. Koeda, T. Omori, R. Kainuma, K. Ishida, K. Oikawa, Appl. Phys. Lett. 85 (2004) 4358.
[2] M. Khan, M.I. Dubenko, S. Stadler, N. Ali, J. Phys.: Condens. Matter 20 (2008) 235204.
[3] T. Krenke, M. Acet, E. Wassermann, X. Moya, L. Manosa, A. Planes, Phys. Rev. B 72 (2005) 014412.
[4] T. Krenke, M. Acet, E. Wassermann, X. Moya, L. Manosa, A. Planes, Phys. Rev. B 73 (2006) 174413.
[5] K. Oikawa, W. Ito, Y. Imano, Y. Sutou, R. Kainuma, K. Ishida, S. Okamoto, O. Kitakami, T. Kanomata, Appl. Phys. Lett. 88 (2006) 122507.
[6] R. Kainuma, Y. Imano, W. Ito, Y. Sutou, H. Morito, S. Okamoto, O. Kitakami, K. Oikawa, A. Fujita, T. Kanomata, K. Ishida, Nature 439 (2006) 957.
[7] R. Kainuma, Y. Imano, W. Ito, H. Morito, Y. Sutou, K. Oikawa, A. Fujita, K. Ishida, S. Okamoto, O. Kitakami, T. Kanomata, Appl. Phys. Lett. 88 (2006) 192513.
[8] S.Y. Yu, L. Ma, G.D. Liu, Z.H. Liu, J.L. Chen, Z.X. Cao, G.H. Wu, B. Zhang, X.X. Zhang, Appl. Phys Lett. 90 (2007) 242501.
[9] R. Kainuma, W. Ito, R.Y. Umetsu, K. Oikawa, K. Ishida, Appl. Phys. Lett. 93 (2008) 091906.
[10] S.Y. Yu, Z.H. Liu, G.D. Liu, J.L. Chen, Z.X. Cao, G.H. Wu, B. Zhang, X.X. Zhang, App. Phys. Lett. 89 (2006) 162503.
[11] V.K. Sharma, M.K. Chattopadhyay, K.H.B. Shaeb, A. Chouhan, S.B. Roy, Appl. Phys. Lett. 89 (2006) 222506.
[12] K. Koyama, H. Okada, K. Watanabe, T. Kanomata, R. Kainuma, W. Ito, K. Oikawa, K. Ishida, Appl. Phys. Lett. 89 (2006) 182510.
[13] T. Krenke, E. Duman, M. Acet, E.F. Wassermann, X. Moya, L. Manosa, A. Planes, Nat. Mater. 4 (2005) 450.
[14] M. Khan, N. Ali, S. Stadler, Appl. Phys. Lett. 101 (2007) 053919.
[15] V.K. Sharma, M.K. Chattopadhyay, S.B. Roy, J. Phys. D: Appl. Phys. 40 (2007) 1869.
[16] W. Ito, K. Ito, R.Y. Umetsu, R. Kainuma, K. Koyama, K. Watanabe, A. Fujita, K. Oikawa, K. Ishida, T. Kanomata, Appl. Phys. Lett. 92 (2008) 021908.
[17] S. Kustov, M.L. Corro, J. Pons, E. Cesari, Appl. Phys. Lett. 94 (2009) 191901.
[18] R.Y. Umetsu, W. Ito, K. Ito, K. Koyama, A. Fujita, K. Oikawa, K. Watanabe, T. Kanomata, R. Kainuma, K. Ishida, Scripta Mater. 60 (2009) 25.
[19] V.K. Sharma, M.K. Chattopadhyay, S.B. Roy, Phys. Rev. B 76 (2007) 140401(R).
[20] X. Xu, W. Ito, R.Y. Umetsu, K. Koyama, R. Kainuma, K. Ishida, Mater. Trans. 51 (2010) 469.
[21] X. Xu, W. Ito, M. Tokunaga, R.Y. Umetsu, R. Kainuma, K. Ishida, Mater. Trans. 51 (2010) 1357.
[22] X. Xu, W. Ito, R.Y. Umetsu, R. Kainuma, K. Ishida, Appl. Phys. Lett. 95 (2009) 181905.
[23] W. Ito, Y. Imano, R. Kainuma, Y. Sutou, K. Oikawa, K. Ishida, Metall. Mater. Trans. A 38 (2007) 759.
[24] H.E. Karaca, I. Karaman, B. Basaran, Y. Ren, Y.I. Chumlyakov, H.J. Maier, Adv. Funct. Mater. 19 (2009) 983.
[25] I.W. Chen, Y.H. Chiao, K. Tsuzaki, Acta Metall. 33 (1985) 1847.
[26] M. Umemoto, W.S. Owen, Met. Trans. 5 (1974) 2041.
[27] F.J. Gil, J.M. Manero, J.A. Planell, J. Mater. Sci. 30 (1995) 2526.
[28] R. Kainuma, F. Gejima, Y. Sutou, I. Ohnuma, K. Ishida, Mater. Trans. JIM 41 (2000) 943.